Electronic Supplementary Information (ESI)

Turn-on and color-switchable red luminescent liquid crystal based on pyrrolopyrrole derivatives

Shuangxiong Dai, Yudai Zhou, Haoli Zhang, Zhengxu Cai, Bin Tong,* Jianbing Shi and Yuping Dong*

Beijing Key Laboratory of Construction Tailorable Advanced Functional Materials and Green Applications, School of Material Science & Engineering, Beijing Institute of Technology, 5 South Zhongguancun Street, Beijing, 100081, China

* To whom correspondence should be addressed.

Phone: +86-10-6891-7390; E-mail: tongbin@bit.edu.cn, chdongyp@bit.edu.cn

Table of Contents

1. Synthesis of the four TPPP derivatives.

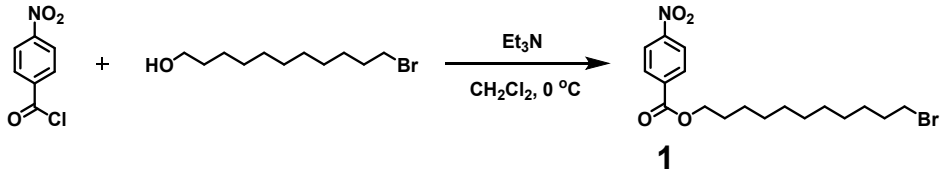

Scheme S1. The synthetic route of compound 1.

Compound 1. In a 100 mL round-bottom flask equipped with magnetic stir bar, 11-bromo-1-undecanol (0.01 mol, 2.51 g), and trimethylamine (0.01 mol, 1.01 g) were placed followed by the addition of CH_2Cl_2 (20 mL). The mixture was stirred and cooled to 0°C, 4-nitrobenzoyl chloride (0.01 mol, 1.86 g) was dissolved in 10 mL CH_2Cl_2 and slowly added to reaction mixture. After the addition completed, the reaction mixture was warmed to room temperature and stirred overnight. The CH_2Cl_2 was evaporated under reduced pressure, the residue was purified by column chromatography on silica gel using ethyl acetate/petroleum ether (1/10, v/v) as the eluent. Yield: 3.44g (86%). ^{1}H NMR (400 MHz, $CDCl_3$, ppm): δ 8.31-8.28 (m, 2H), 8.23-8.19 (m, 2H), 4.37 (t, J = 6.80 Hz, 2H), 3.41 (t, J = 6.80 Hz, 2H), 1.89-1.76 (m, 4H), 1.48-1.25 (m, 14H); ^{13}C NMR (101 MHz, $CDCl_3$, ppm): δ 164.77, 150.51, 135.90, 130.67, 123.53, 66.11, 34.04, 32.81, 29.45, 29.43, 29.39, 29.23, 28.75, 28.61, 28.16, 25.98; MALDI-TOF-MS (*m*/*z*) calcd. for $C_{18}H_{26}BrNO_4$ $[M]^+$: 399.10, found: 400.10.

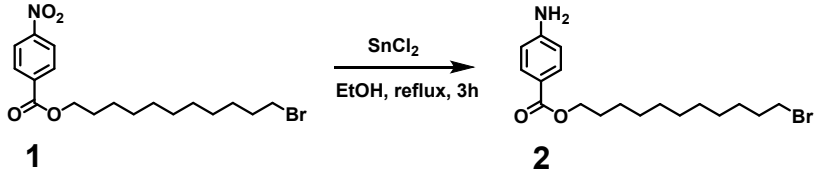

Scheme S2. The synthetic route of compound 2.

Compound 2. In a 250 mL round-bottom flask equipped with magnetic stir bar, **compound 1** (0.01 mol, 4.00 g) and $SnCl_2 \cdot 2H_2O$ (0.05 mol, 11.30 g) were placed followed by the addition of EtOH (80 mL). The mixture was stirred and heating refluxed 3 h. After that time, the reaction mixture was then cooled to room temperature. Aqueous $NaHCO_3$ was slowly added and the mixture was extracted with CH_2Cl_2. The organic layers were combined, then dried over Na_2SO_4. The solvent was removed under reduced pressure and the resulting crude product was purified by column chromatography on silica gel using ethyl acetate/petroleum ether (1/7, v/v) as the eluent. Yield: 3.07g (83%). ^{1}H NMR (400 MHz, DMSO-d_6, ppm): δ 7.64-7.61 (m, 2H), 6.58-6.54 (m, 2H), 4.14 (t, J = 6.80 Hz, 2H), 3.51 (t, J = 6.80 Hz, 2H), 1.81-1.74 (m, 2H), 1.68-1.61

(m, 2H), 1.40-1.26 (m, 14H); ^{13}C NMR (101 MHz, DMSO-d_6, ppm): δ 166.36, 153.85, 131.46, 116.56, 113.13, 63.96, 35.63, 32.72, 29.35, 29.32, 29.13, 28.83, 28.57, 27.99, 26.01. MALDI-TOF-MS (*m*/*z*) calcd. for $C_{18}H_{28}BrNO_2$ $[M]^+$: 369.13, found: 370.10.

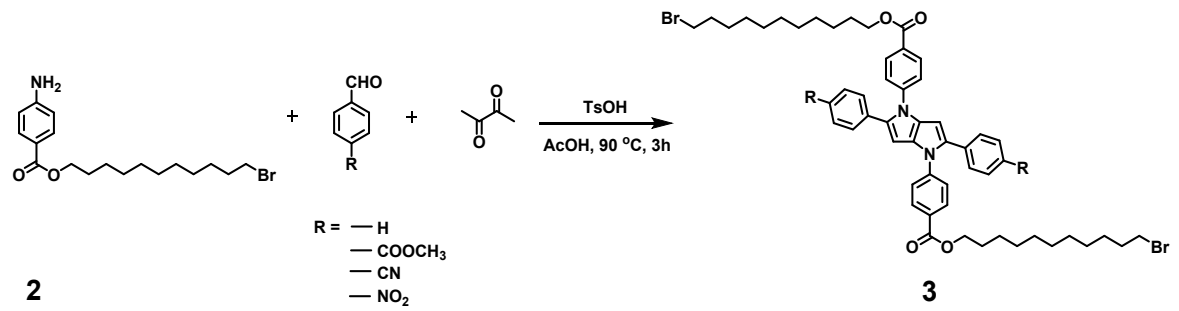

Scheme S3. The synthetic route of intermediates 3.

Intermediates 3. In a 50 mL round-bottom flask equipped with magnetic stir bar, **compound 2** (0.01 mol, 3.70 g), aldehyde (0.01 mol), and *p*-toluenesulphonic acid (0.001 mol, 0.17 g) were placed followed by the addition of glacial acetic acid (25 mL). The mixture was stirred at 90 °C for 30 min. After that time, butane-2,3-dione (0.005 mol, 0.43 g) was slowly added via syringe and the resulting mixture was stirred at 90 °C for 3 h. The precipitate of the obtained dye was isolated by filtration and washed with glacial acetic acid. The residue was purified by column chromatography on silica gel using dichloromethane/petroleum ether (2/1, v/v) as the eluent.

Compound 3a: R = –H. ^{1}H NMR (400 MHz, $CDCl_3$, ppm): δ 8.05-8.02 (m, 4H), 7.34-7.31 (m, 4H), 7.29-7.20 (m, 10H, mixed with $CDCl_3$ residual signal), 6.47 (s, 2H), 4.31 (t, J = 6.80 Hz, 4H), 3.40 (t, J = 6.80 Hz, 4H), 1.88-1.72 (m, 8H), 1.46-1.25 (m, 32H); ^{13}C NMR (101 MHz, $CDCl_3$, ppm): δ 166.15, 143.70, 136.04, 133.20, 131.29, 130.65, 128.44, 128.33, 127.40, 126.74, 124.39, 96.43, 65.24, 34.05, 32.83, 29.48, 29.46, 29.41, 29.29, 28.76, 28.18, 26.06; MALDI-TOF-MS (*m*/*z*) calcd. for $C_{54}H_{64}Br_2N_2O_4$ $[M]^+$: 964.32, found: 965.30.

Compound 3b: R = –COOCH$_3$. ^{1}H NMR (400 MHz, $CDCl_3$, ppm): δ 8.08-8.05 (m, 4H), 7.93-7.91 (m, 4H), 7.34-7.30 (m, 4H), 7.28-7.26 (m, 4H, mixed with $CDCl_3$ residual signal), 6.56 (s, 2H), 4.33 (t, J = 6.40 Hz, 4H), 3.90 (s, 6H), 3.40 (t, J = 6.80 Hz, 4H), 1.88-1.73 (m, 8H), 1.46-1.25 (m, 32H); ^{13}C NMR (101 MHz, $CDCl_3$, ppm): δ 166.80, 165.94, 143.28, 137.31, 135.73, 132.55, 130.89, 129.76, 128.03, 127.71, 124.59, 97.28, 65.35, 52.12, 34.04, 32.83, 29.72, 29.47, 29.40, 29.28, 28.75, 28.17, 26.05; MALDI-TOF-MS (*m*/*z*) calcd. for $C_{58}H_{68}Br_2N_2O_8$ $[M]^+$: 1080.33, found 1081.30.

Compound 3c: R = –CN. ^{1}H NMR (400 MHz, $CDCl_3$, ppm): δ 8.12-8.08 (m, 4H), 7.54-7.51 (m, 4H), 7.33-7.28 (m, 8H), 6.55 (s, 2H), 4.34 (t, J = 6.80 Hz, 4H), 3.40 (t, J = 6.80 Hz, 4H), 1.89-1.74 (m, 8H), 1.47-1.25 (m, 32H); ^{13}C NMR (101 MHz, $CDCl_3$, ppm): δ 165.79, 142.86, 137.11, 135.20, 133.00, 132.25, 131.08, 128.54, 128.12, 124.66, 118.81, 109.93, 97.65, 65.48, 34.05, 32.82, 29.72, 29.48, 29.45, 29.40, 29.27, 28.75, 28.16, 26.04; MALDI-TOF-MS (*m*/*z*) calcd. for $C_{56}H_{62}Br_2N_4O_4$ $[M]^+$: 1014.31, found: 1015.30.

Compound 3d: R = –NO_2. Yield: 0.92 g (17%). ^{1}H NMR (400 MHz, $CDCl_3$, ppm) δ 8.13-8.10 (m, 8H), 7.36-7.32 (m, 8H), 6.61 (s, 2H), 4.34 (t, J = 6.80 Hz, 4H), 3.40 (t, J = 6.80 Hz, 4H), 1.88-1.74 (m, 8H), 1.47-1.25 (m, 32H); ^{13}C NMR (101 MHz, $CDCl_3$, ppm): δ 165.72, 146.01, 142.76, 138.95, 135.23, 133.52, 131.17, 128.76, 128.01, 124.76, 123.96, 98.05, 65.51, 34.05, 32.81, 29.72, 29.48, 29.45, 29.40, 29.27, 28.74, 28.15, 26.04. MALDI-TOF-MS (*m*/*z*) calcd. for $C_{54}H_{62}Br_2N_4O_8$ $[M]^+$: 1054.29, found: 1055.30.

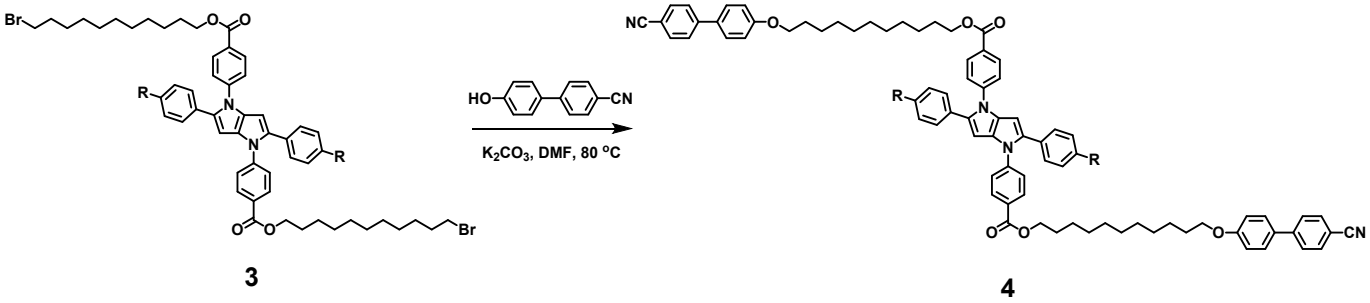

Scheme S4. The synthetic route of TPPP derivatives 4.

TPPP derivatives 4. In a 50 mL round-bottom flask equipped with magnetic stir bar, **compound 3** (0.50 mmol), 4'-hydroxy-4-biphenylcarbonitrile (1.50 mmol, 0.29 g), and K_2CO_3 (1.50 mmol, 0.21 g) were placed followed by the addition of DMF (25 mL). The mixture was stirred at 80 °C for 12 h. After that time, the reaction mixture was cooled to room temperature and water was added. The resulting aqueous layer was extracted with CH_2Cl_2. The organic layers were combined, then dried over Na_2SO_4. The solvent was removed under reduced pressure and the resulting crude product was purified by column chromatography on silica gel using dichloromethane/ethyl acetate (100/1, v/v) as the eluent.

Compound 4a: R = –H. ^{1}H NMR (400 MHz, $CDCl_3$, ppm): δ 8.05-8.01 (m, 4H), 7.69-7.62 (m, 8H), 7.53-7.50 (m, 4H), 7.34-7.40 (m, 4H), 7.29-7.19 (m, 10H, mixed with $CDCl_3$ residual signal), 7.00-6.96 (m, 4H), 6.47 (s, 2H), 4.31 (t, J = 6.80 Hz, 4H), 4.00 (t, J = 6.40 Hz, 4H), 1.84-1.73 (m, 8H), 1.51-1.24 (m, 28H);

^{13}C NMR (101 MHz, $CDCl_3$, ppm): δ 166.14, 159.82, 145.30, 143.69, 136.03, 133.18, 132.58, 131.28, 130.66, 128.44, 128.33, 127.40, 127.08, 126.74, 124.38, 119.14, 115.09, 110.06, 96.43, 68.18, 65.25, 29.54, 29.51, 29.38, 29.29, 29.23, 28.76, 26.05; MALDI-TOF-MS (*m*/*z*) calcd. for $C_{80}H_{80}N_4O_6$ $[M]^+$: 1192.61, found: 1192.60; Elemental analysis calcd. (%) for $C_{80}H_{80}N_4O_6$: C 80.51, H 6.76, N 4.69, O 8.04, found C 80.48, H 6.85, N 4.60, O 8.07.

Compound 4b: R = –COOCH$_3$. ^{1}H NMR (400 MHz, $CDCl_3$, ppm) δ 8.08-8.05 (m, 4H), 7.93-7.90 (m, 4H), 7.70-7.67 (m, 4H), 7.65-7.62 (m, 4H), 7.53-7.50 (m, 4H), 7.33-7.30 (m, 4H), 7.28-7.26 (m, 4H, mixed with $CDCl_3$ residual signal), 7.00-6.96 (m, 4H), 6.55 (s, 2H), 4.33 (t, J = 6.8 Hz, 4H), 4.00 (t, J = 6.40 Hz, 4H), 3.90 (s, 6H), 1.84-1.74 (m, 8H), 1.51-1.24 (m, 28H); ^{13}C NMR (101 MHz, $CDCl_3$, ppm): δ 166.79, 165.93, 159.81, 145.29, 143.27, 137.29, 135.73, 132.58, 132.54, 131.27, 130.90, 129.76, 128.33, 128.05, 128.03, 127.71, 127.08, 124.58, 119.13, 115.09, 110.06, 97.28, 68.18, 65.36, 52.12, 29.55, 29.52, 29.39, 29.29, 29.23, 28.75, 26.05; MALDI-TOF-MS (*m*/*z*) calcd. for $C_{84}H_{84}N_4O_{10}$ $[M]^+$: 1308.62, found: 1308.60. Elemental analysis calcd. (%) for $C_{80}H_{80}N_4O_6$: C 77.04, H 6.47, N 4.28, O 12.22, found C 76.96, H 6.63, N 4.11, O 12.30.

Compound 4c: R = –CN. ^{1}H NMR (400 MHz, $CDCl_3$, ppm): δ 8.11-8.09 (m, 4H), 7.69-7.62 (m, 8H), 7.53-7.48 (m, 8H), 7.32-7.27 (m, 8H), 7.00-6.97 (m, 4H), 6.55 (s, 2H), 4.34 (t, J = 6.40 Hz, 4H), 4.00 (t, J = 6.80 Hz, 4H), 1.84-1.74 (m, 8H), 1.51-1.24 (m, 28H); ^{13}C NMR (101 MHz, $CDCl_3$, ppm): δ 165.78, 159.81, 145.28, 142.85, 137.10, 135.19, 132.99, 132.58, 132.26, 131.28, 131.08, 128.54, 128.34, 128.12, 127.08, 124.65, 119.13, 118.82, 115.10, 110.06, 109.92, 97.67, 68.18, 65.49, 29.54, 29.40, 29.31, 29.24, 28.75, 26.06; MALDI-TOF-MS (*m*/*z*) calcd. for $C_{82}H_{78}N_6O_6$ $[M]^+$: 1242.60, found: 1242.60. Elemental analysis calcd. (%) for $C_{80}H_{80}N_4O_6$: C 79.20, H 6.32, N 6.76, O 7.72, found C 79.11, H 6.55, N 6.57, O 7.77.

Compound 4d: R = –NO$_2$. ^{1}H NMR (400 MHz, $CDCl_3$, ppm): δ 8.14-8.09 (m, 8H), 7.69-7.62 (m, 8H), 7.54-7.50 (m, 4H), 7.35-7.31 (m, 8H), 7.00-6.96 (m, 4H), 6.61 (s, 2H), 4.34 (t, J = 6.80 Hz, 4H), 4.00 (t, J = 6.40 Hz, 4H), 1.84-1.75 (m, 8H), 1.51-1.25 (m, 28H); ^{13}C NMR (101 MHz, $CDCl_3$, ppm): δ 165.71, 159.82, 146.02, 145.28, 142.76, 138.94, 135.24, 133.52, 132.57, 131.29, 131.17, 128.77, 128.33, 128.00, 127.08, 124.76, 123.95, 119.11, 115.11, 110.08, 98.05, 68.18, 65.51, 56.57, 29.52, 29.38, 29.29, 29.23, 28.75, 26.05; MALDI-TOF-MS (*m*/*z*) calcd. for $C_{80}H_{78}N_6O_{10}$ $[M]^+$: 1282.58, found: 1282.60. Elemental analysis calcd. (%) for $C_{80}H_{80}N_4O_6$: C 74.86, H 6.13, N 6.55, O 12.46, found C 74.68, H 6.35, N 6.47, O

12.50.

2. Preparation of TPPP-NO_2-mixed PDMS thin film.

We used Sylgard 184 from Dow Corning as the precursor to make the TPPP-NO_2-mixed PDMS thin film. It was prepared by mixing the silicone base (part A), the curing agent (part B), and the ground TPPP-NO_2 powder at 1000:100:1 weight ratio. The mixture was fully stirred and degassed until all of the air bubbles were removed. Finally, they were poured into a clean container and cured at 80 °C in an oven for 3 h to obtained TPPP-NO_2-mixed PDMS thin film.

3. Photophysical properties of the four TPPP derivatives.

Table S1. Photophysical properties of the four TPPP derivatives in solution and solid states.

Comps	Solution (THF)					Solid				
	Abs/nm	Em/nm	Stoke's shift/nm	Φ_F/%	τ/ns	Abs/nm	Em/nm	Stoke's shift/nm	Φ_F/%	τ/ns
TPPP-H	309,372	509	137	6.08	2.13	315,375	455	80	50.38	5.66
TPPP-MF	294,396	466	70	86.13	1.61	303,407	501	94	21.70	1.02
TPPP-CN	295,399	461	62	84.68	1.53	303,414	516	102	10.03	0.92
TPPP-NO_2	294,455	592	137	6.05	0.51	301,481	610	129	0.10	–

4. Density functional theory (DFT) calculations.

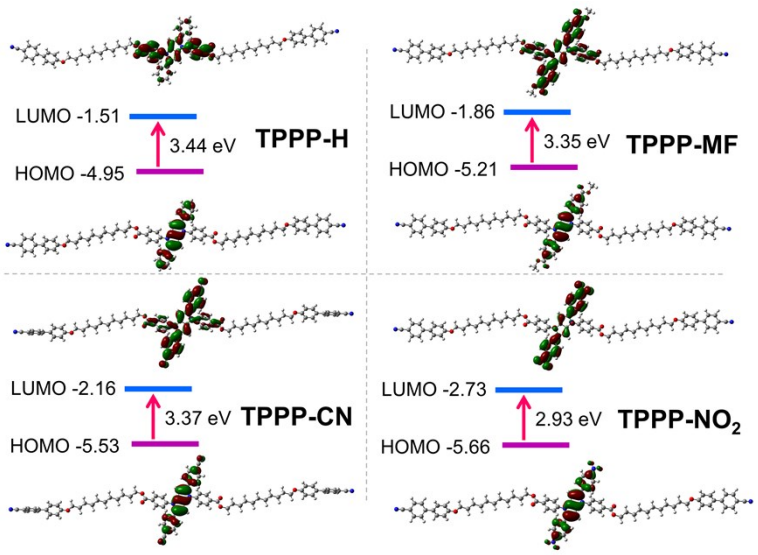

Figure S1. Calculated electron distributions of HOMOs–LUMOs and the energy levels of the four TPPP

derivatives.

5. Aggregation behaviors in THF/water mixtures.

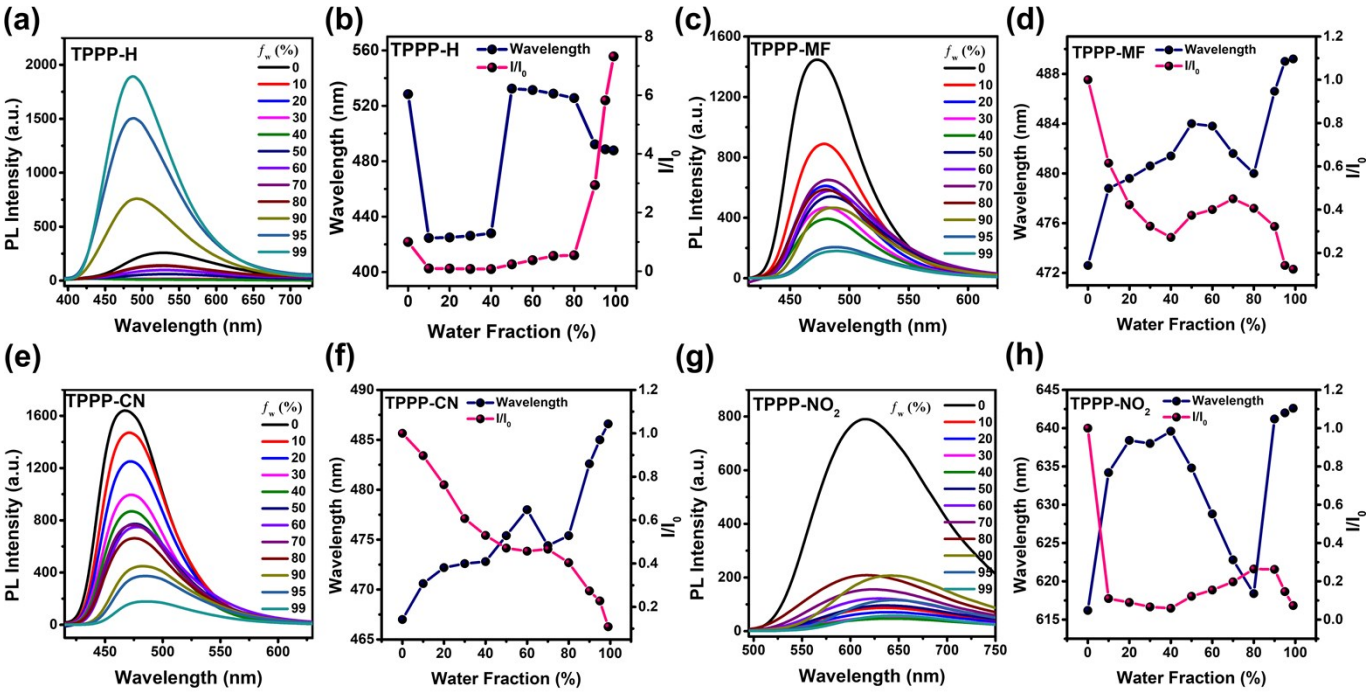

Figure S2. Fluorescence spectra of the four TPPP derivatives in THF/water mixtures with different water fractions (a, c, e, g). The plot of wavelength and the ratio of maximum fluorescence intensity vs. water fraction (b, d, f, h). I_0 = emission intensity in pure THF solution. Concentration: 0.01 mM.

6. Time-resolved PL decays spectra.

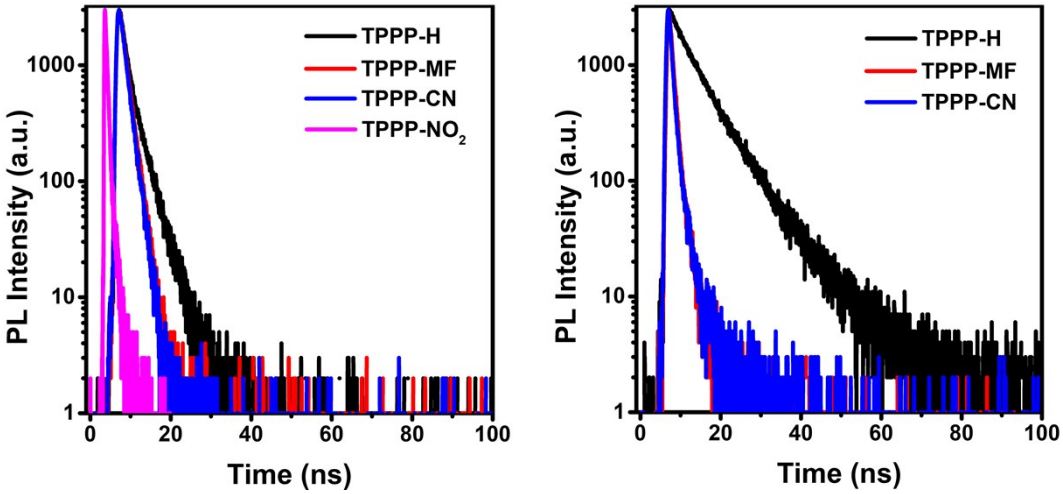

Figure S3. Time-resolved PL decays spectra of the four TPPP derivatives measured in THF solution (left, 0.01 mM) and solid states (right). All profiles were taken at room temperature.

7. TGA test of the four TPPP derivatives and DSC curves of TPPP-H, TPPP-MF and TPPP-CN.

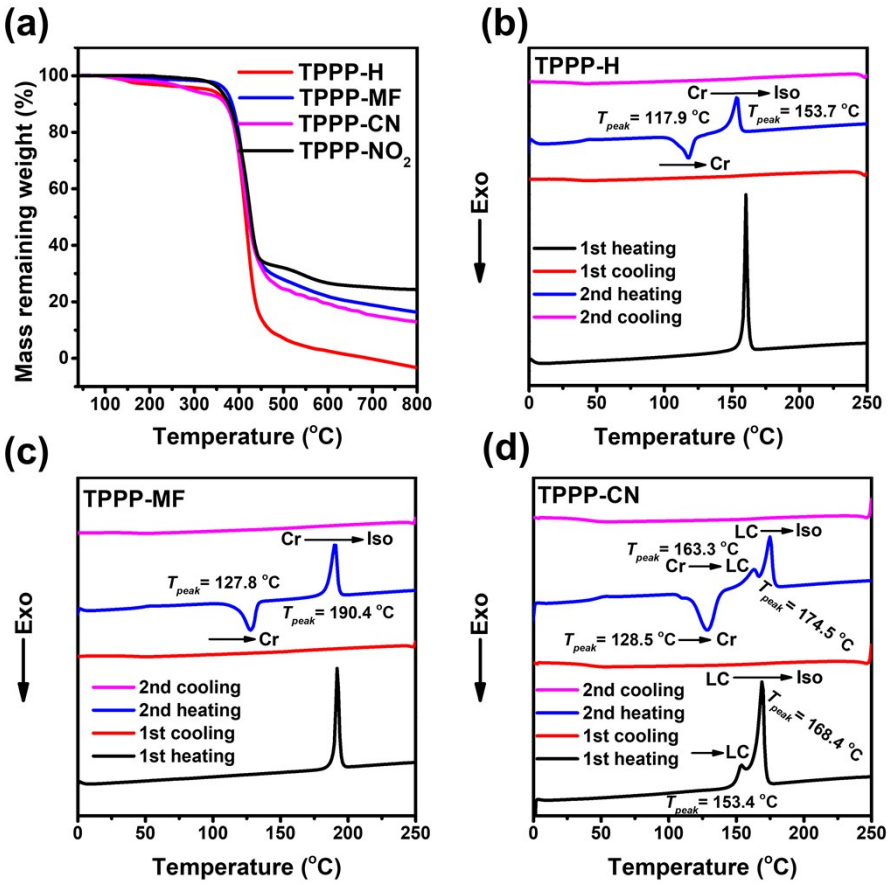

Figure S4. (a) TGA thermograms of the four TPPP derivatives measured under nitrogen at a heating rate of 10 °C/min. DSC curves of TPPP-H (b), TPPP-MF (c) and TPPP-CN (d) recorded under nitrogen with a scan rate of 10 °C/min.

8. POM images of TPPP-NO_2 in LC state and glass state.

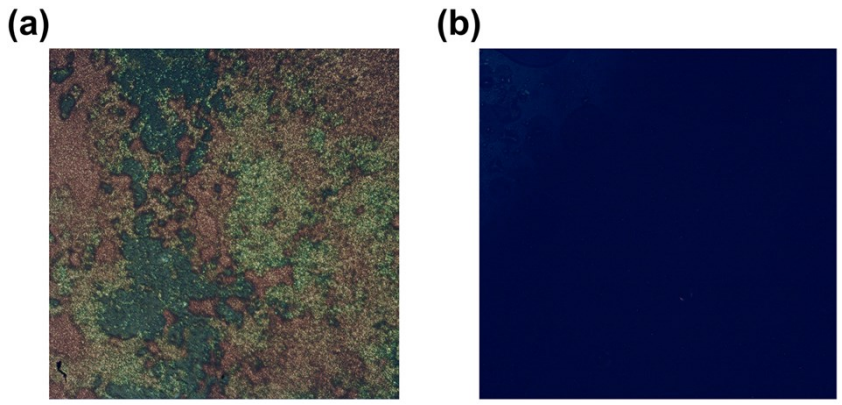

Figure S5. (a) Mesomorphic textures of TPPP-NO_2 observed by POM via heating the sample to 155 °C

with a rate of 5 °C min^{-1} on the first heating cycles; (b) The dark-field of TPPP-NO_2 observed by POM in the glass state on the cooling process.

9. XRD curve and mesomorphic textures of TPPP-CN in the LC phase.

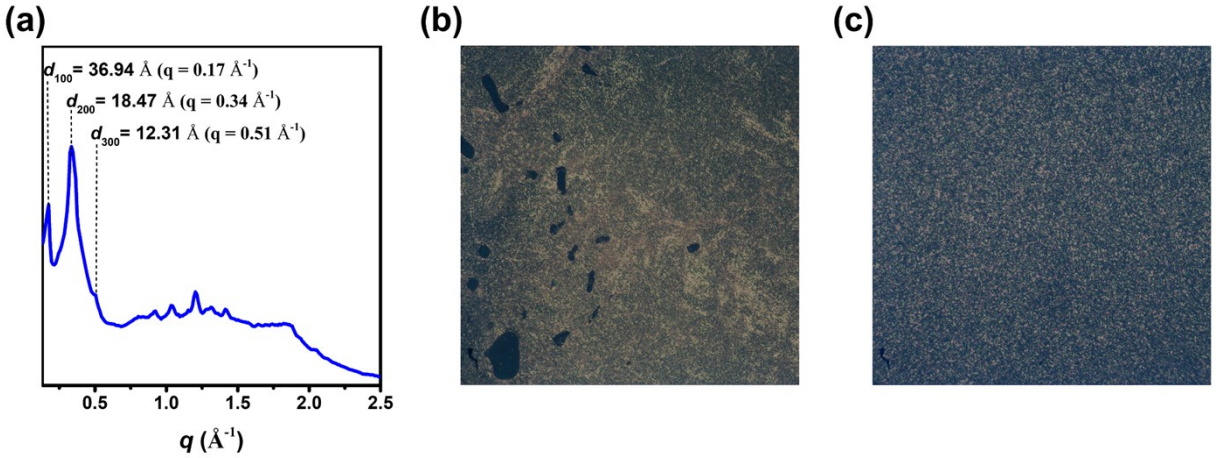

Figure S6. (a) 1D XRD curve of TPPP-CN measured by heating the sample to 168 °C with a rate of 3 °C min^{-1}; Mesomorphic texture of TPPP-CN observed by POM via heating the sample with a rate of 3 °C min^{-1} to 165 °C on the first heating cycles (b) and 170 °C on the second heating cycles (c).

10. ^{13}C NMR, in-situ FT-IR, and UV-vis spectra of TPPP-NO_2 in different states.

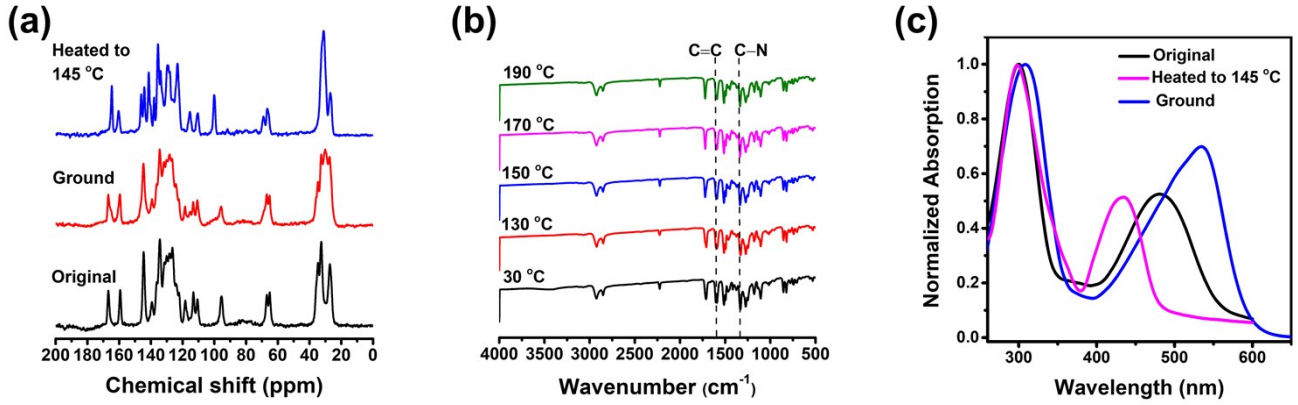

Figure S7 (a) ^{13}C NMR spectra of TPPP-NO_2 in different states; (b) In-situ FT-IR spectra of TPPP-NO_2 on the heating process from the original state; (c) UV-vis spectra of TPPP-NO_2 in different solid states.

11. Temperature-dependent photophysical properties of grinded TPPP-NO_2.

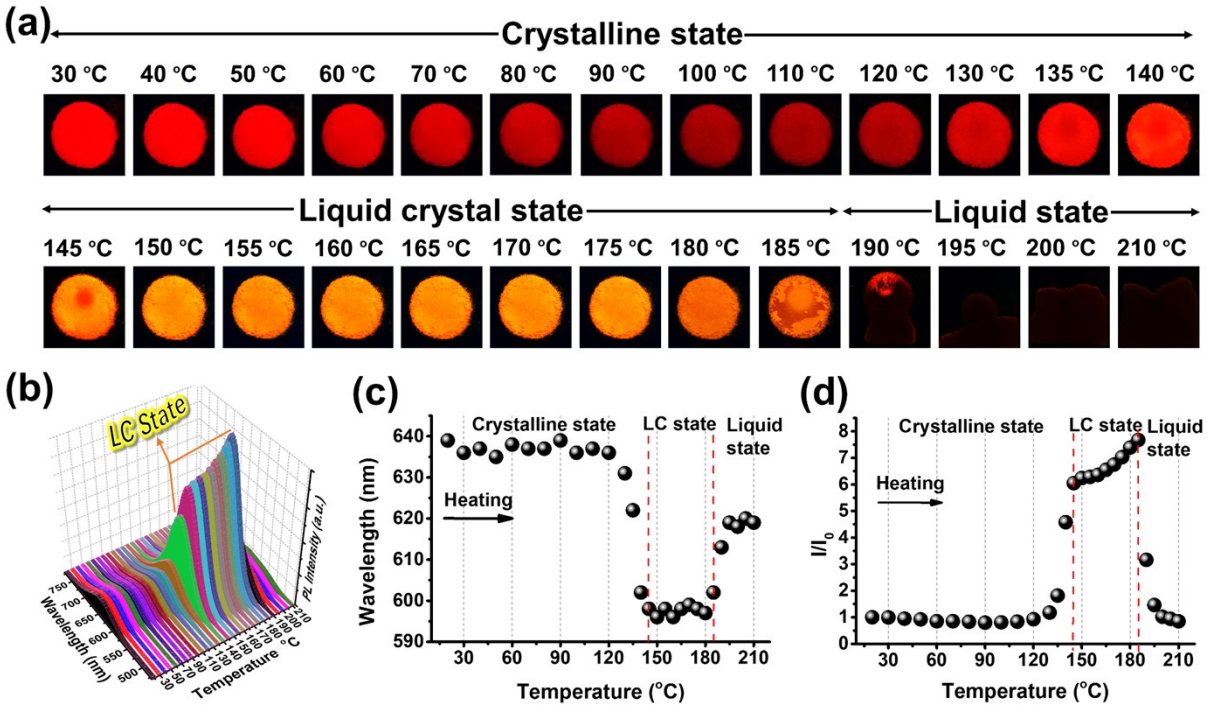

Figure S8. (a) Photos of TPPP-NO_2 during the heating process from 30 to 210 °C under 365 nm UV light. (b) Temperature-dependent fluorescence spectra at the heating process. Corresponding PL wavelength maximum shift behaviors (c) and PL intensity change behaviors (d).

12. DSC curves of grinded TPPP-NO_2.

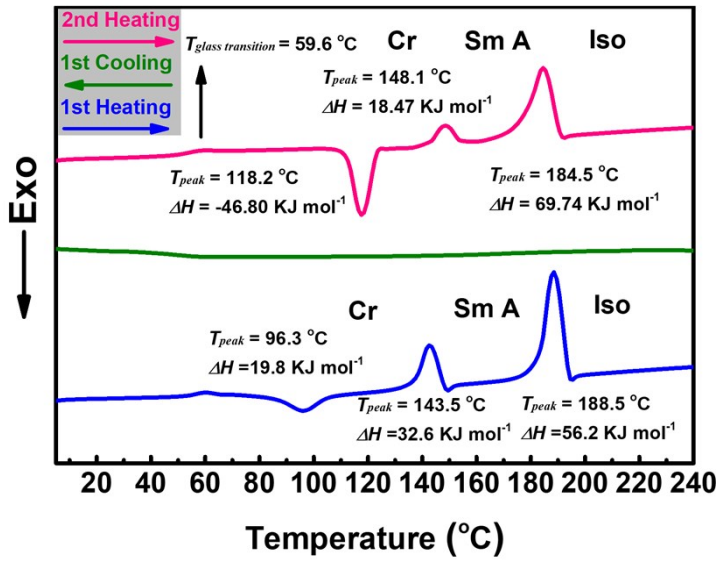

Figure S9. DSC curves of ground TPPP-NO_2 with a scan rate of 10 °C min^{-1} under nitrogen.

13. ^{1}H NMR, ^{13}C NMR and MALDI-TOF-MS spectra of the TPPP derivatives.

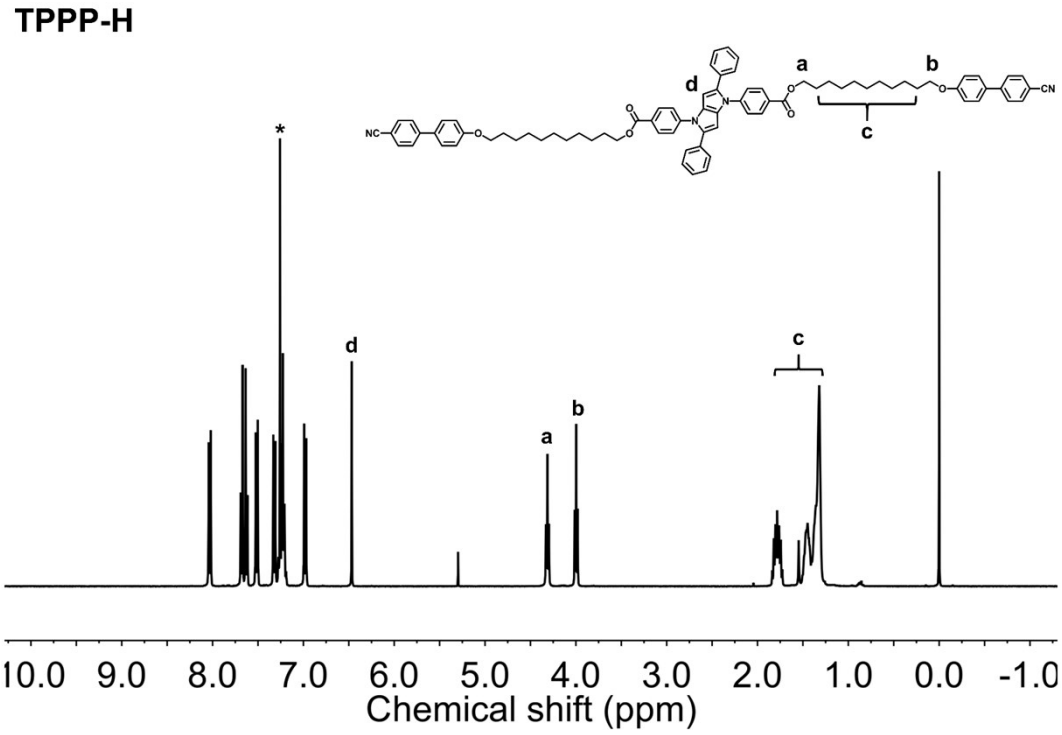

Figure S10. ^{1}H NMR spectra of TPPP-H in $CDCl_3$.

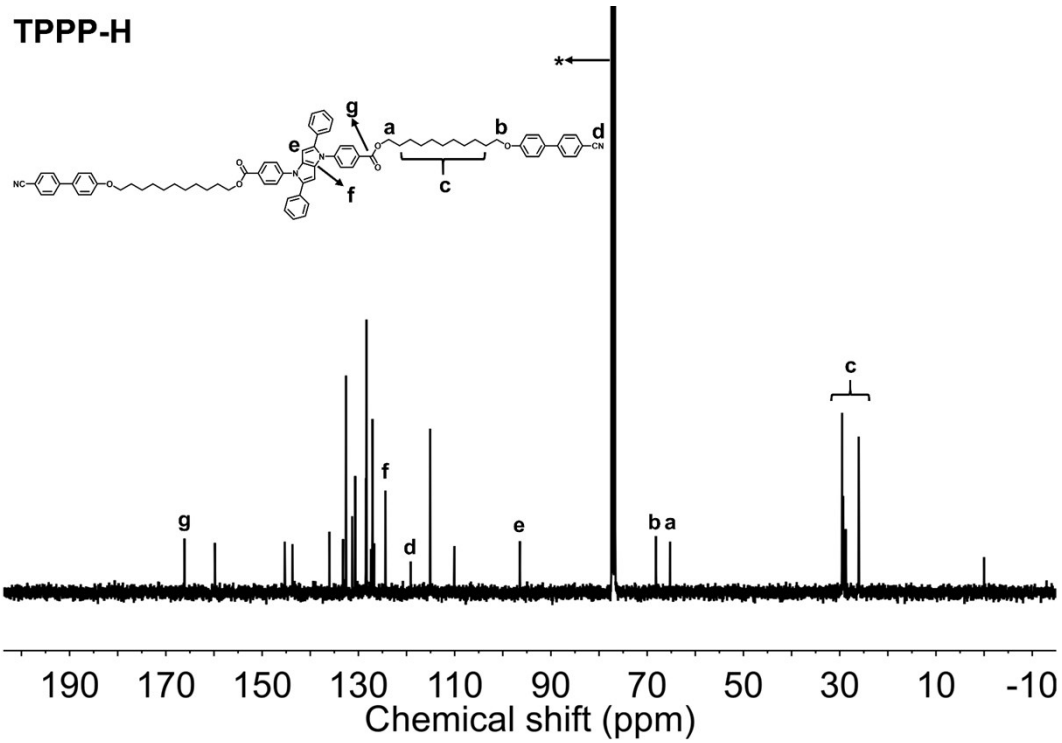

Figure S11. ^{13}C NMR spectra of TPPP-H in $CDCl_3$.

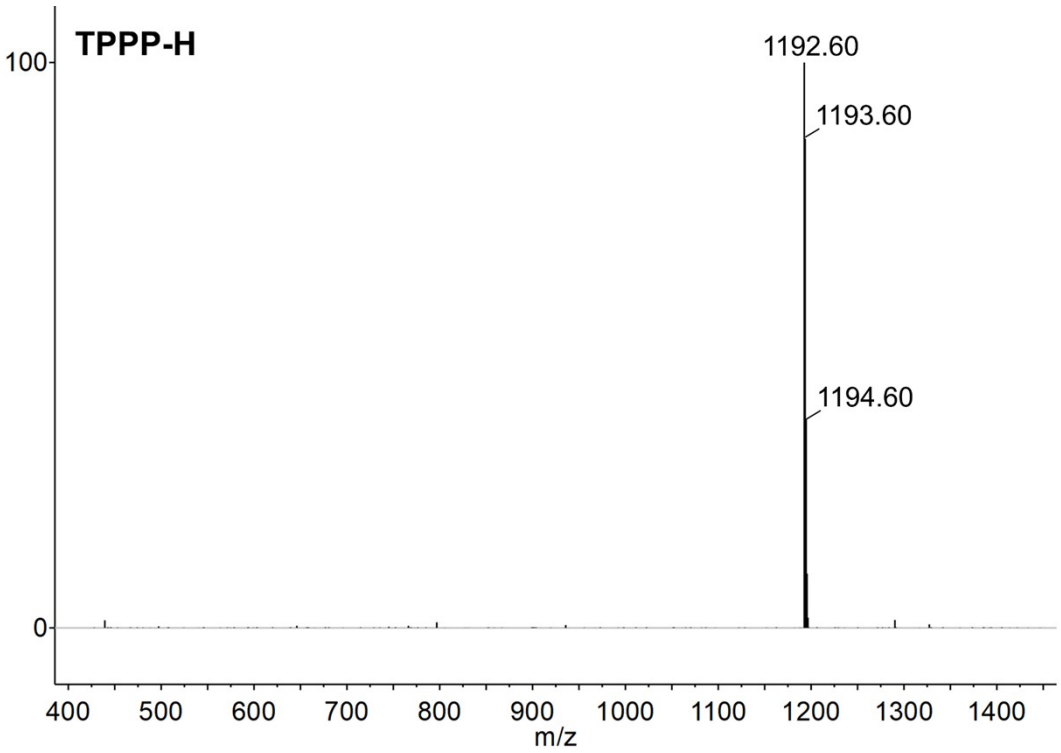

Figure S12. MALDI-TOF-MS spectra of TPPP-H.

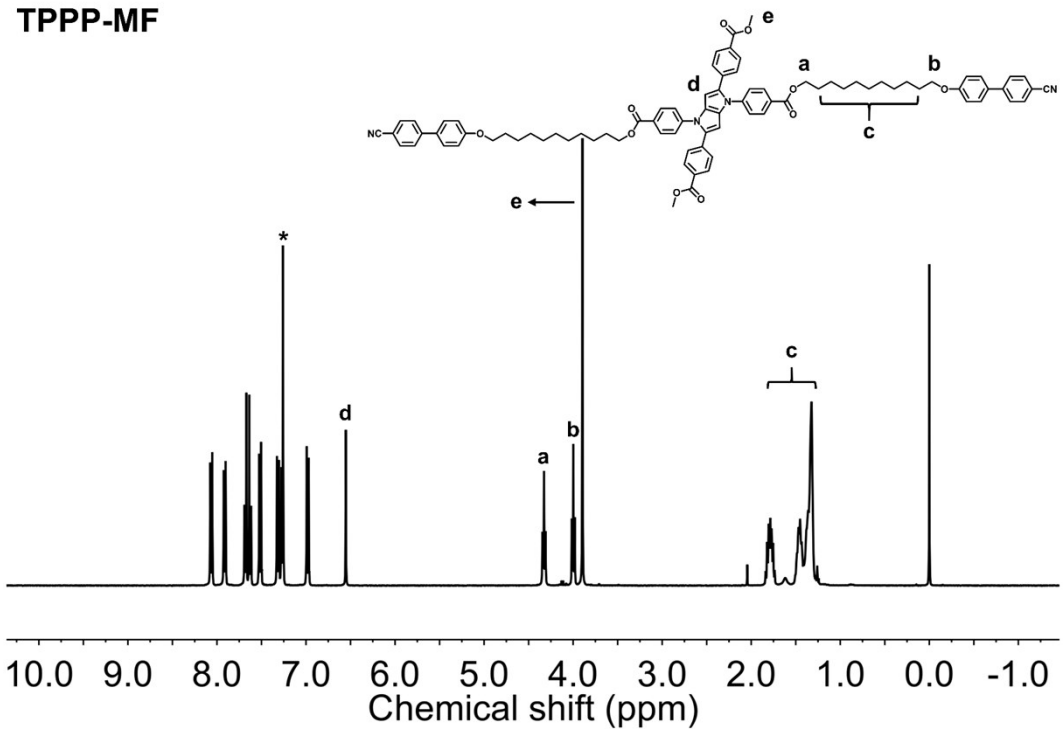

Figure S13. ^{1}H NMR spectra of TPPP-MF in $CDCl_3$.

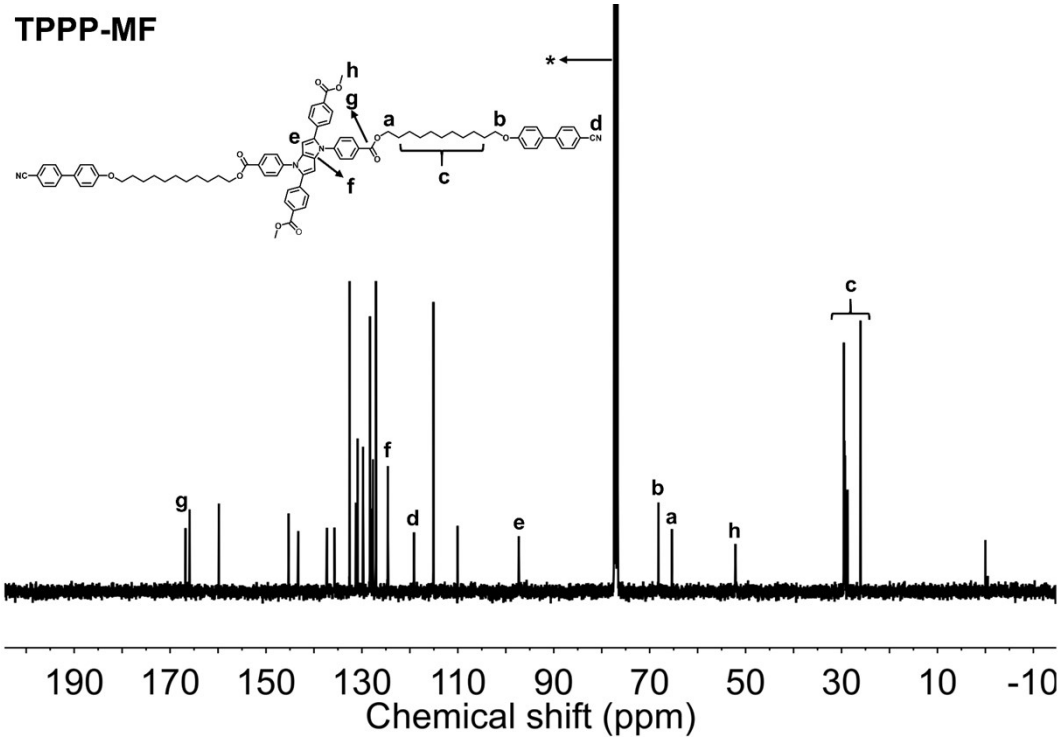

Figure S14. ^{13}C NMR spectra of TPPP-MF in $CDCl_3$.

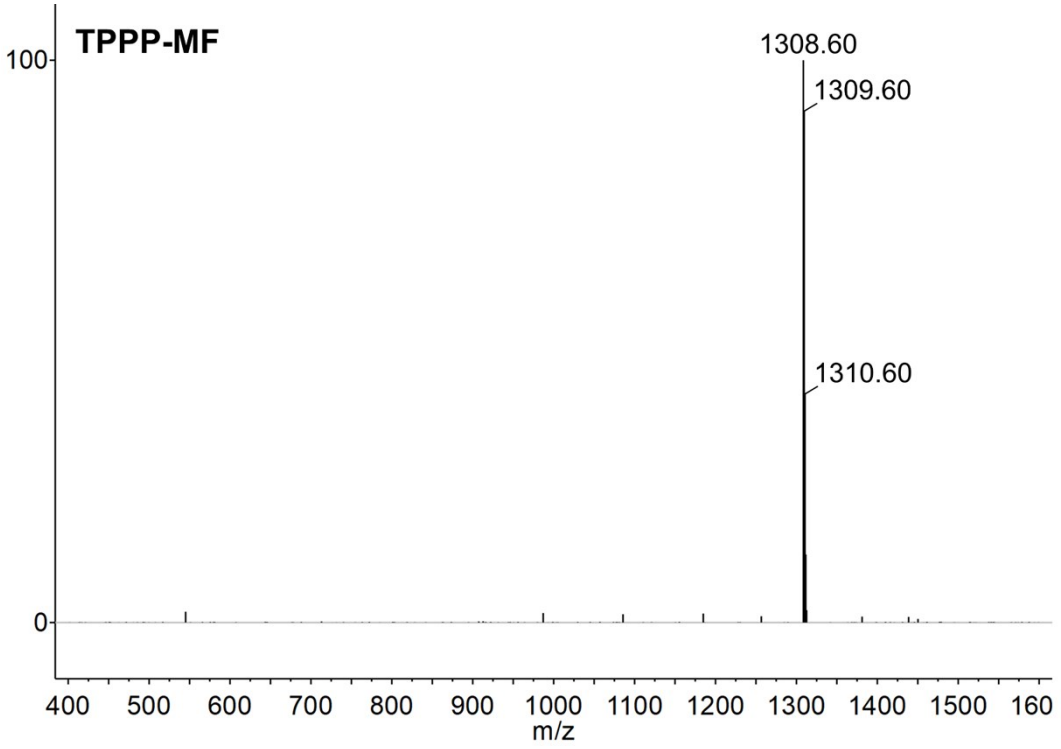

Figure S15. MALDI-TOF-MS spectra of TPPP-MF.

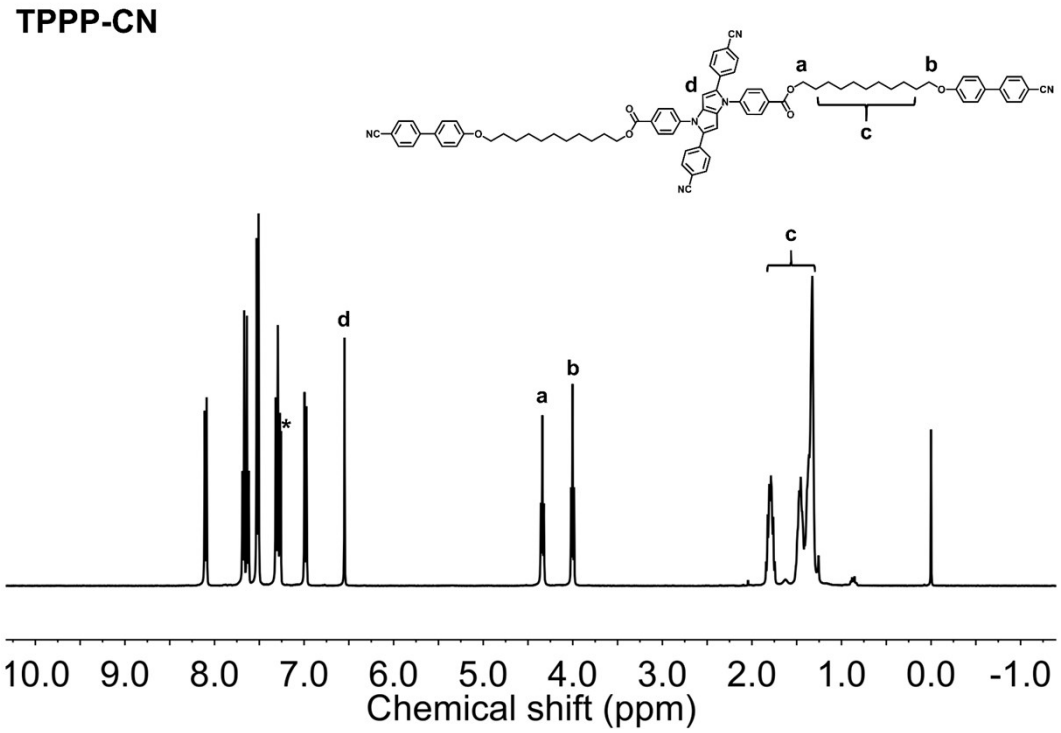

Figure S16. ^{1}H NMR spectra of TPPP-CN in $CDCl_3$.

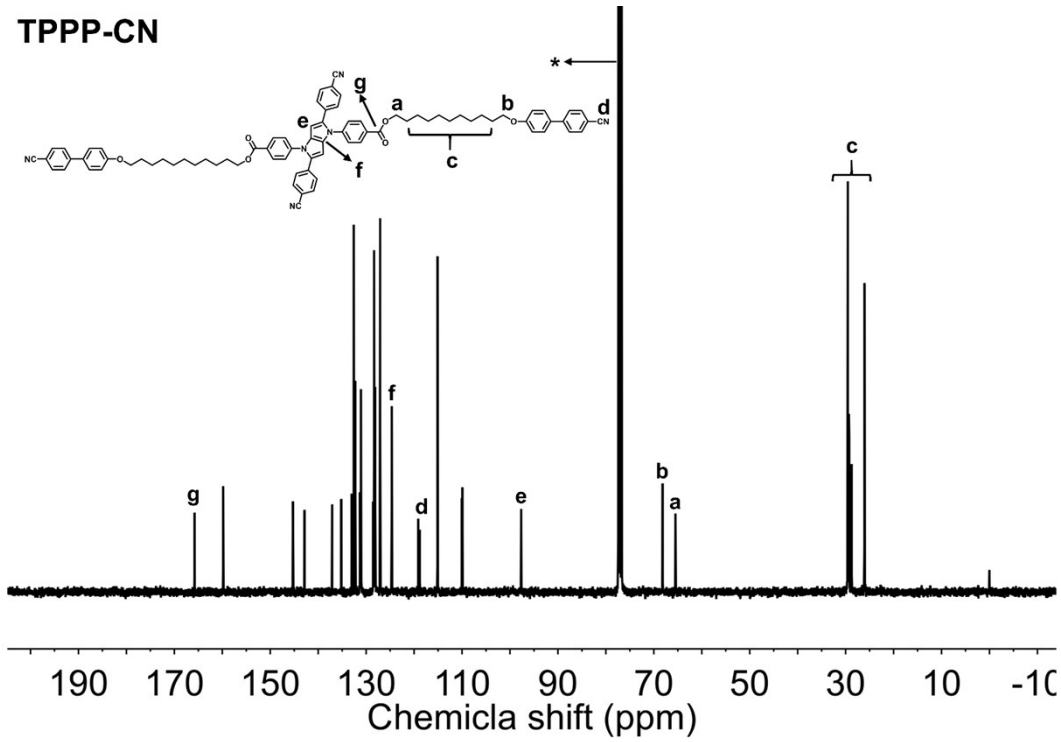

Figure S17. ^{13}C NMR spectra of TPPP-CN in $CDCl_3$.

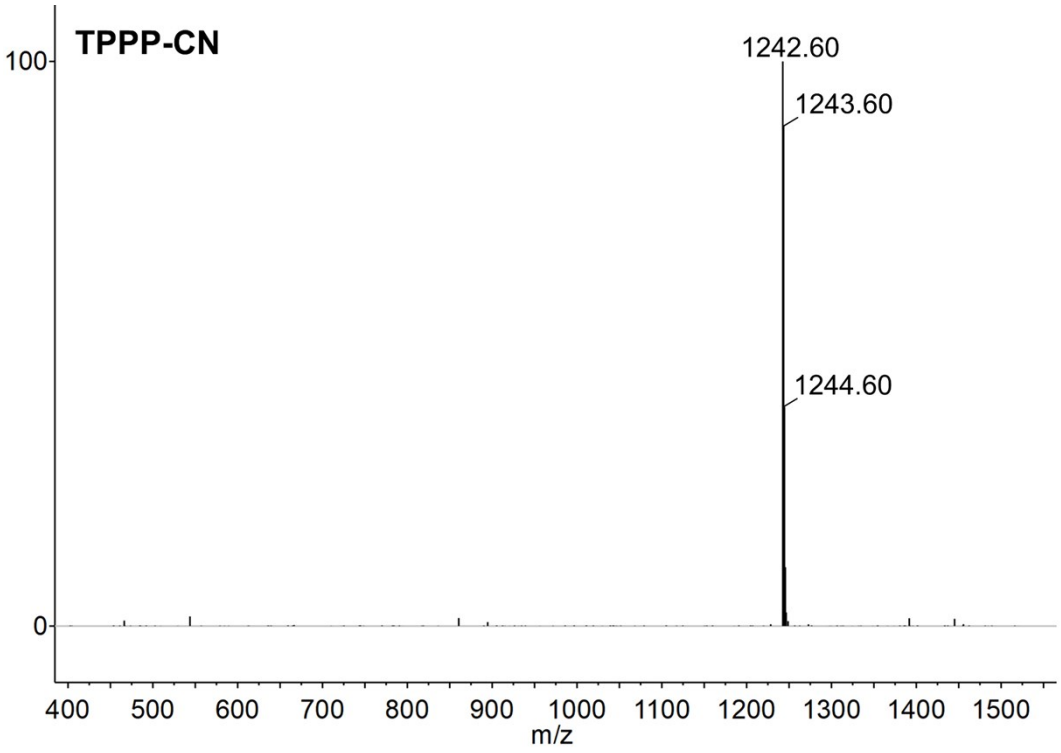

Figure S18. MALDI-TOF-MS spectra of TPPP-CN.

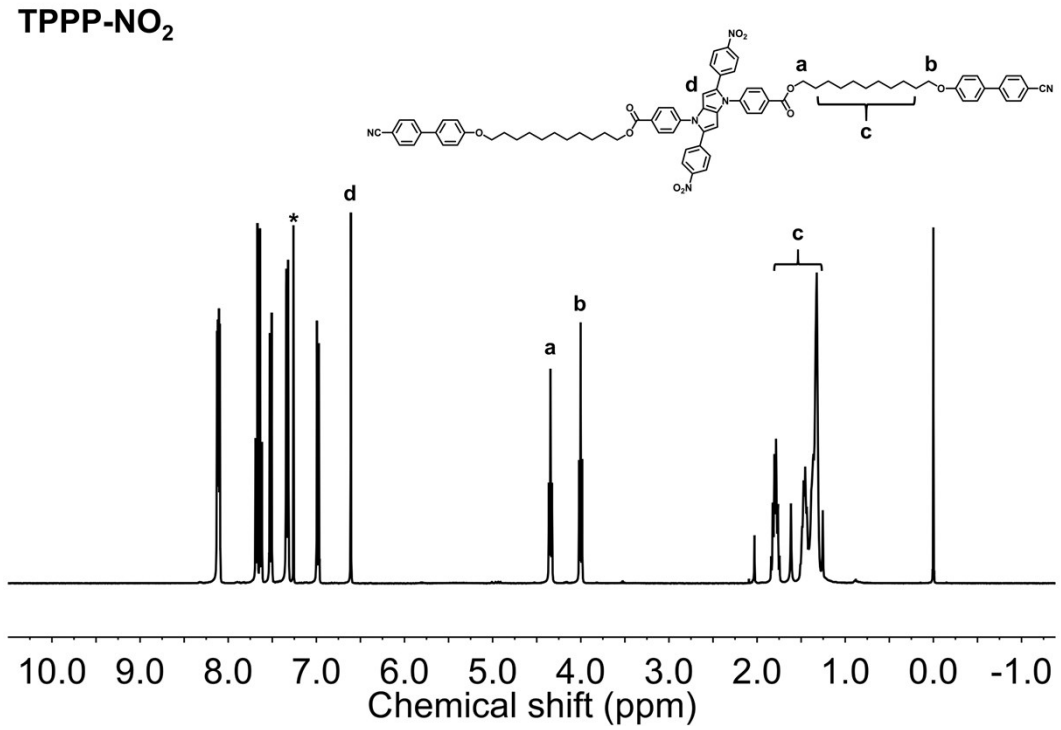

Figure S19. ^{1}H NMR spectra of TPPP-NO_2 in $CDCl_3$.

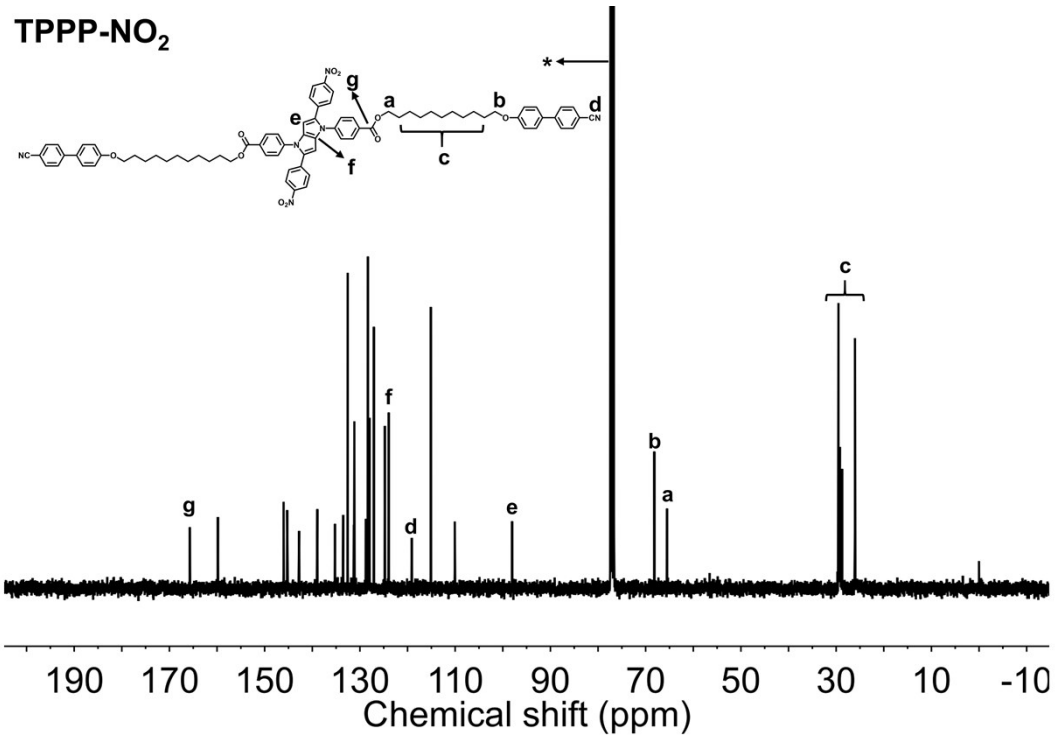

Figure S20. ^{13}C NMR spectra of TPPP-NO_2 in $CDCl_3$.

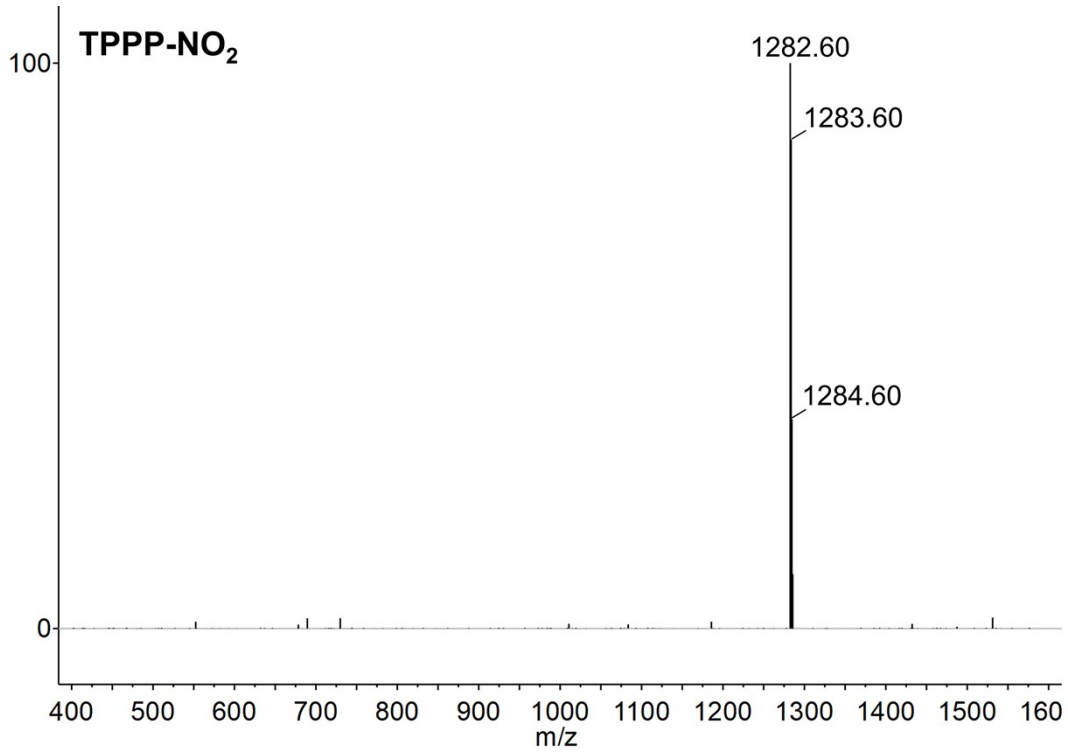

Figure S21. MALDI-TOF-MS spectra of TPPP-NO_2.